XLIII CILAMCE
21-25, November, 2022
FOZ DO IGUAÇU – PR – BRAZIL

Application of a hybrid method for forecast time series in concrete deformation in a counterstruct dam

Lucas da Silva Ribeiro[1], Samuel Bellido dos Santos [1], Jairo Marlon Correa[1], Tásia Hickmann[1], Étore Funchal de Faria [2]

[1]*Dep. Academic of Mathematic and Statistic, Federal Technological University of Paraná - UTFPR, Medianeira (PR), Brasil*
prof.lucasribeiro@gmail.com, jairocorrea@utfpr.edu.br, hickmann@utfpr.edu.br, samuelb@utfpr.edu.br
[2]*Itaipu Binacional, Foz do Iguaçu (PR), Brasil*
etore@itaipu.gov.br

Abstract. The concrete deformations have been researchers study object in the structural safety of dams process. These deformations, which occur over time, are influenced by various physical and environmental factors. One of the environmental factors that affect the deformations of concrete is the ambient temperature. In this paper, a hybrid method called SARIMAX-NEURAL is presented for prediction of concrete deformations that are influenced by ambient temperature. This hybrid method was defined as a linear combination of predictions from Box & Jenkins methodology models and Deep Learning neural network models with Long Short-Term Memory architecture. Historical data of concrete deformations were measured by rosettes strain installed in a buttress block in the Itaipu dam for a period of 34 years. The proposed hybrid method, which considered the effect of ambient temperature on the deformations of concrete, effective results presented in comparison with the individual methods in which the effect was not considered to ambient temperature. The predictive accuracy gains were between 25% and 60%.

Keywords: Time series. Deep Learning Neural Networks. Box & Jenkins models.

1 Introduction

Phenomenon that occurs in concrete, over time, deformations and have been the object of research worldwide from the second half of the twentieth century in civil construction, in general, and in concrete dams of hydroelectric plants. Deformations are considered a highly complex phenomenon due to the many factors that influence it, such as: geometric factors – dimensions of the concrete structure; environmental factors – ambient temperature and relative air humidity; concrete mass aggregates - water/cement ratio [1].

This paper presents a hybrid method in time series, called SARIMAX-NEURAL, to model and predict the deformations of concrete taking into account the effects of ambient temperature on them, with historical data from deformimeter rosettes installed in the D57 buttress block of the Itaipu hydroelectric plant.

This hybrid method was defined as the linear combination, that is, the sum of the predictions of the Autoregressive Integrated Moving Averages methods with exogenous variables (SARIMAX) and the Deep Learning (DL) Recurrent Neural Networks (RNN) method with Long Short-Term Memory (LSTM) architecture.

2 Theoretical Reference

2.1 Concrete Deformations

The study of concrete deformations has been the object of research by researchers for decades. The deformation produced by drying was studied by Gerald Pickett in the 1940s and became known as the Pickett effect ([2] apud [3]). This effect can be controlled in sealed specimens, but in constructions such as concrete dams the Pickett effect cannot be disregarded (as is the case with the Itaipu dam). [4] says that the Pickett effect corresponds to creep by drying.

According to [4], in concrete under loading there are three main types of deformations over time: elastic deformations - always reversible; visco-elastic deformations - partially reversible, with an elastic phase and a viscous phase; plastic deformations - always irreversible. Elastic deformation has an instantaneous and a retarded part - in instantaneous elastic deformation the stress-strain relationship is governed by Hooke's Law, but retarded elastic deformation is time-dependent. According to NBR6118 the total deformation of concrete is composed of three parts: immediate deformation, creep deformation and shrinkage deformation. For [5] concrete deformations are affected by five factors, as shown in Table 1.

Table 1 - Factors that influence in the deformations of concrete over time

Groups	**Factors**
Environmental factors	Relative humidity, air temperature, ventilation and solar radiation
Material factors	Cement type, A/C ratio, % paste, additives, aggregates and f_{ck}
Geometric factors	Shape and medium thickness
Mechanic factors	Charging intensity
Temporal factors	Age of the concrete Concrete Age at Charging Time of charging

According to [6] since 1982 several mathematical models have been proposed for modeling concrete creep and shrinkage. The most cited are: The B3 model [7], GL2000 model [8], Eurocode 2 EC2 model [9], NBR6118 model [10] and ACI model [11]. Each of these models has its own complexity regarding the amount of input data, considering the different characteristics of each type of concrete. It should be noted that in these models the design data are used for the simulations of the deformation curves, but in the hybrid time series method presented in this paper, the data for numerical simulation are real concrete deformation data. At the Itaipu hydroelectric plant, concrete creep is measured, as follows [12].

2.2 Times Series: Box & Jenkins Methodology

The Box & Jenkins methodology was developed with the objective of identifying a probabilistic model from a stationary second-order time series, that is, with constant mean and variance. That is, the data must have a linear self-dependence or autocorrelation structure between time series values [13]. The ARMA(p,q) model for a stationary Z_t time series is composed of the Autoregressive AR(p) and Moving Average MA(q) models, where p is the number of autoregressive parameters (taking p previous values to define the prediction) and q is the number of moving average parameters (taking the average of the errors of the p autoregressive values). This model is represented by:

$$\left(1-\phi_1 B-\phi_2 B^2-\ldots-\phi_p B^p\right) Z_t = \delta + \left(1-\theta_1 B-\theta_2 B^2-\ldots-\theta_q B^q\right) a_t \tag{1}$$

Where ϕ_1, ϕ_2, ..., ϕ_p e θ_1, θ_2, ..., θ_q are the parameters, autoregressive and moving averages, respectively, to be determined, δ is a constant of the model and a_t is the error or random shock.

If the time series presents seasonality, then the statistical model can be said to be multiplicative SARIMA(p,d,q)(P,D,Q)s, where P is the auto regressive order of the seasonal part, D is the difference order of the seasonal part (if the series is not stationary) and Q is the number of moving average parameters of the seasonal period s. The order of the p, q, and d parameters is identified by analyzing the profile plots of the Autocorrelation Function (*ACF*) and Partial Autocorrelation Function (*PACF*) according to [14]. The SARIMA model for a non-stationary time series Z_t with seasonality is defined by the equation:

$$\phi(B)\Phi(B^s)(1-B^s)^D(1-B)^d Z_t = \theta(B)\Theta(B^s)\, a_t \tag{2}$$

The univariate Box & Jenkins methodology also allows the use of exogenous variables (or explanatory variables) in the composition of the adjusted model, making it possible to study the impact of these variables on the prediction model. The inclusion of exogenous variables X_r in model (2) generates the model SARIMAX(p,d,q,r)x(P,D,Q)$_s$, [15], defined by:

$$\phi(B)\Phi(B^s)(1-B^s)^D(1-B)^d Z_t = \delta + \theta(B)\Theta(B^s)a_t + \beta\left(1-B\right)^d X_r \tag{3}$$

where, β are the coefficients of the exogenous variables X_r.

being

i) B is backward translation operator or delay operator, m values, defined as $B^m Z_t = Z_{t-m}$;

ii) $\phi(\mathrm{B}) = 1-\phi_1 B - \ldots - \phi_p B^p$ is non-seasonal autoregressive part, in polynomial form, of order p;

iii) $\Phi(\mathrm{B}^s) = 1-\Phi_1 B^s - \ldots - \Phi_p B^{Ps}$ is the seasonal autoregressive part of order P and seasonal order s;

iv) $(1-B^s)^D$ is the seasonal differentiation operator of order D and seasonal order s;

v) $(1-B)^d$ is the non-seasonal differentiation operator of order d;

vi) $\theta(\mathrm{B}) = 1-\theta_1 B - \ldots - \theta_q B^q$ is the non-seasonal part of moving averages, in polynomial form, of order q;

vii) $\Theta(\mathrm{B}^s) = 1-\Theta_1 B^s - \ldots - \Theta_Q B^{Qs}$ is the seasonal part of Q-order moving averages and seasonal s.

2.3 Recurrent neural networks deep learning (RNN-DL)

Being a class of neural networks that includes weighted connections within a hidden layer, forming loops that can store information when processing new inputs, Deep Learning networks with LSTM architecture create a long internal short-term memory in which previous inputs are considered as data from the time series itself [16]. In one-way or feed-forward neural networks called Feed-forward neural networks, there is only one path to take: from input to output. There is no feedback (loops), that is, the output of any hidden layer does not affect the same layer. Recurrent or feedbacked neural networks, on the other hand, can have synaptic signals traveling in both directions, introducing loops in the network. Computations derived from previous input are fed back into the network, giving them a kind of "short memory". Their "state" changes continuously until it reaches an equilibrium point, remaining at that point until the input changes and a new equilibrium is found [17].

The practical effect of this is that there is short-term memory in the net, but for a long period of time. Considering learning by training a kind of long-term memory, then recurrent neural nets can create much more complex models capable of solving a wider range of problems [18]. It is important to note that Deep Learning neural networks with Long Short-Term Memory (LSTM) architecture are suitable for prediction of sequential time series [19].

3 Materials and Method

For this paper, the historical data (of a 34-year period) of corrected concrete deformations and ambient temperature were made available by Itaipu and measured by deformimeter rosettes installed in the D57 buttress block. It was necessary to transform the historical data into time series by means of cubic spline, redistributing the

data on a weekly basis. The SARIMAX-NEURAL hybrid method presented in this paper is applicable to seasonal time series with exogenous variables and its modeling has two phases: in the first phase, modeling is performed by the SARIMAX model to predict the linear component of the prediction; in the second phase, modeling is performed, in the series of residuals from the SARIMAX model, via recurrent deep learning neural networks with LSTM architecture, called (RNN DL-LSTM) to predict the non-linear component of the prediction.

Generically, the linear and nonlinear predictive components, respectively, for a time series $Z_t = \{z_t\}_{t=1}^{N}$ can be denoted by:

$$z_t = CL(t) + NL(t) \tag{4}$$

Thus, the hybrid method prediction was obtained as a linear combination (sum) of the out-of-sample prediction (of the linear and nonlinear components) and represented by:

$$\hat{z}_f(t+h) = \overline{CL}_f(t) + \overline{NL}_f(t) \tag{5}$$

Where $\overline{CL}_f(t)$ is the linear component of the prediction (outside the training sample) and $\overline{NL}_f(t)$ is the nonlinear component corresponding to the prediction (outside the training sample) of the time series of the in-sample SARIMAX method residuals, that are represented by:

$$\hat{e}_a(t) = z_{ta} - \hat{z}_{ta} \tag{6}$$

Where z_{ta} is real value and $\hat{z}_{ta}$ is value predicted within the sample. Thus, $\overline{NL}_f(t)$ is prediction, by recurrent neural networks deep learning with LSTM architecture, of the data series of equation (6), with the prediction horizon h = 52 weeks ahead.

4 Results and Discussion

The predictions obtained by the SARIMAX-NEURAL hybrid method were compared with the predictions of the individual SARIMAX, SARIMA and RNN DL-LSTM methods. To verify the accuracy of the predictions three adherence statistics were used: *Mean Absolute Error* (*MAE*), *Mean Absolute Percentage Error* (*MAPE*) e *Root Mean Square Error* (*RMSE*), [14], defined by:

$$MAE = \frac{1}{N}\sum_{t=1}^{N}\left|z(t) - \hat{z}(t)\right| \tag{7}$$

$$MAPE = \frac{1}{N}\sum_{t=1}^{N}\left|\frac{z(t) - \hat{z}(t)}{z(t)}\right| \tag{8}$$

$$RMSE = \sqrt{\frac{1}{N}\sum_{t=1}^{N}\left(z(t) - \hat{z}(t)\right)^2} \tag{9}$$

For this paper, data from rosette RD-D-09 is located upstream of buttress block D57 were used. The data were measured over the period from June of 1981 to December of 2017 standardized weekly by Cubic Spline, as they were originally on a different time scale. 1828 sample data were used for fitting the individual SARIMA, SARIMAX and RNN DL-LSTM methods, in the predictions a prediction horizon h = 52 was used, i.e. 52 steps or weeks ahead. In the Fig. 1 shows the time series of corrected concrete deformations of the five deformimeters (arms) of the RD-D09 deformimeter rosette of the D57 buttress block of the Itaipu hydroelectric power plant.

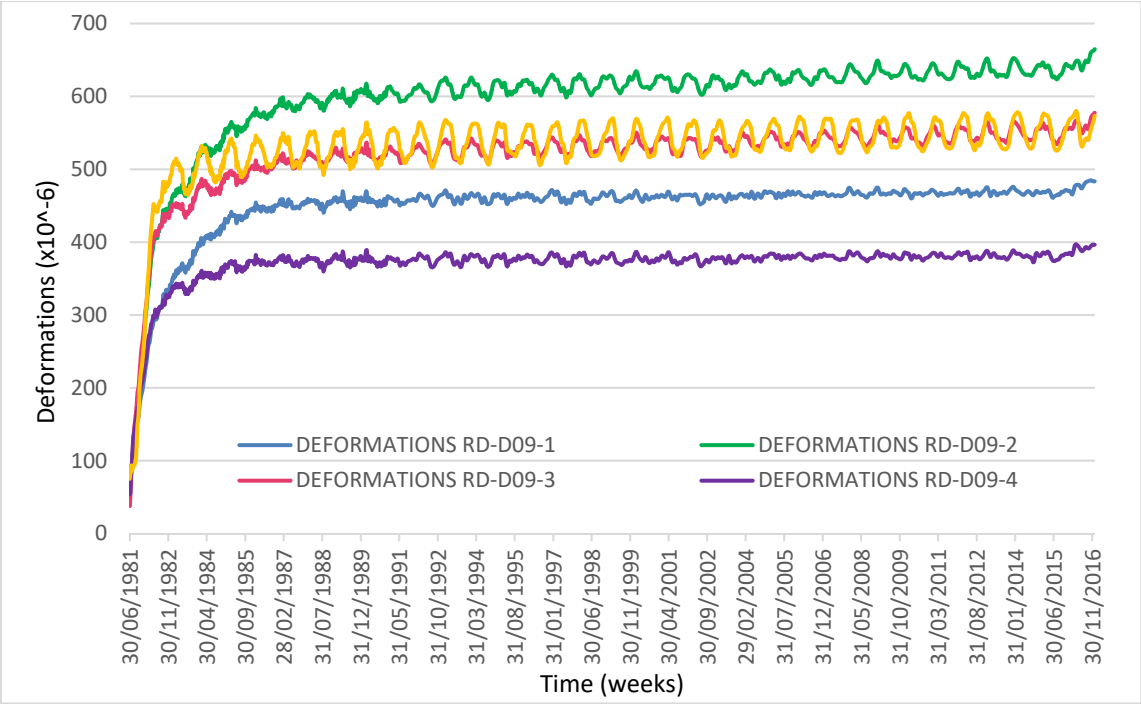

Figure 1 - Time series of corrected concrete deformations of the RD-D09 deformimeter rosette

The parameters of the fitted SARIMAX(p,d,q)x$(P,D,Q)_{52}$ model were determined using the *R* software. The order of the parameters of the automatic model was chosen by the Akaike Information Criterion (AIC) and adjusted by the MAE, MAPE and RMSE criteria on the training sample. Modeling via recurrent neural networks RNN DL-LSTM was in Matlab software, applied to the SARIMAX model residuals. Predictions were calculated for a prediction horizon $h = 52$ weeks ahead.

TABELA 2 - Comaparação da precisão das predições por diferentes métodos preditivos para a roseta RD-D09

MÉTODO	**ROSETA RD-D09-1**			**MÉTODO**	**ROSETA RD-D09-2**		
	MAE	**MAPE**	**RMSE**		**MAE**	**MAPE**	**RMSE**
SARIMA(2,2,3)(0,0,2)	8,34	1,74	9,10	SARIMA(4,2,5)(1,1,0)	16,82	2,59	18,83
RNN DL-LSTM	8,66	1,81	9,39	RNN DL-LSTM	5,70	0,87	7,26
SARIMAX(4,2,3)(0,1,1)	1,31	1,52	7,98	SARIMAX(0,2,1)(1,1,1)	8,57	1,31	9,80
SARIMAX-NEURAL	**4,51**	**0,94**	**516**	SARIMAX-NEURAL	**6,92**	**1,06**	**7,86**
MÉTODO	**ROSETA RD-D09-3**			**MÉTODO**	**ROSETA RD-D09-4**		
	MAE	**MAPE**	**RMSE**		**MAE**	**MAPE**	**RMSE**
SARIMA(2,2,4)(1,1,0)	17,26	3,06	19,34	SARIMA(5,2,4)(0,0,1)	1,29	0,22	2,04
RNN DL-LSTM	9,95	1,39	9,38	RNN DL-LSTM	4,03	1,03	4,64
SARIMAX(0,2,1)(1,1,1)	8,39	1,49	9,79	SARIMAX(4,2,3)(0,1,2)	3,75	0,95	4,51
SARIMAX-NEURAL	**5,35**	**0,94**	**6,12**	SARIMAX-NEURAL	**3,28**	**0,83**	**4,03**
MÉTODO	**ROSETA RD-D09-5**						
	MAE	**MAPE**	**RMSE**				
SARIMA(2,2,2)(1,1,0)	7,78	1,39	9,68				
RNN DL-LSTM	8,58	1,53	9,71				
SARIMAX(4,1,4)(1,1,1)	6,44	1,14	7,04				
SARIMAX-NEURAL	**5,47**	**0,96**	**6,29**				

The Figure 2 show parts of the corrected concrete deformation series and their predictions by the hybrid SARIMAX-NEURAL method and the individual SARIMAX, SARIMA and RNN DL-LSTM methods for arms 1, 2, 4 and 5 of the RD-D09 rosette.

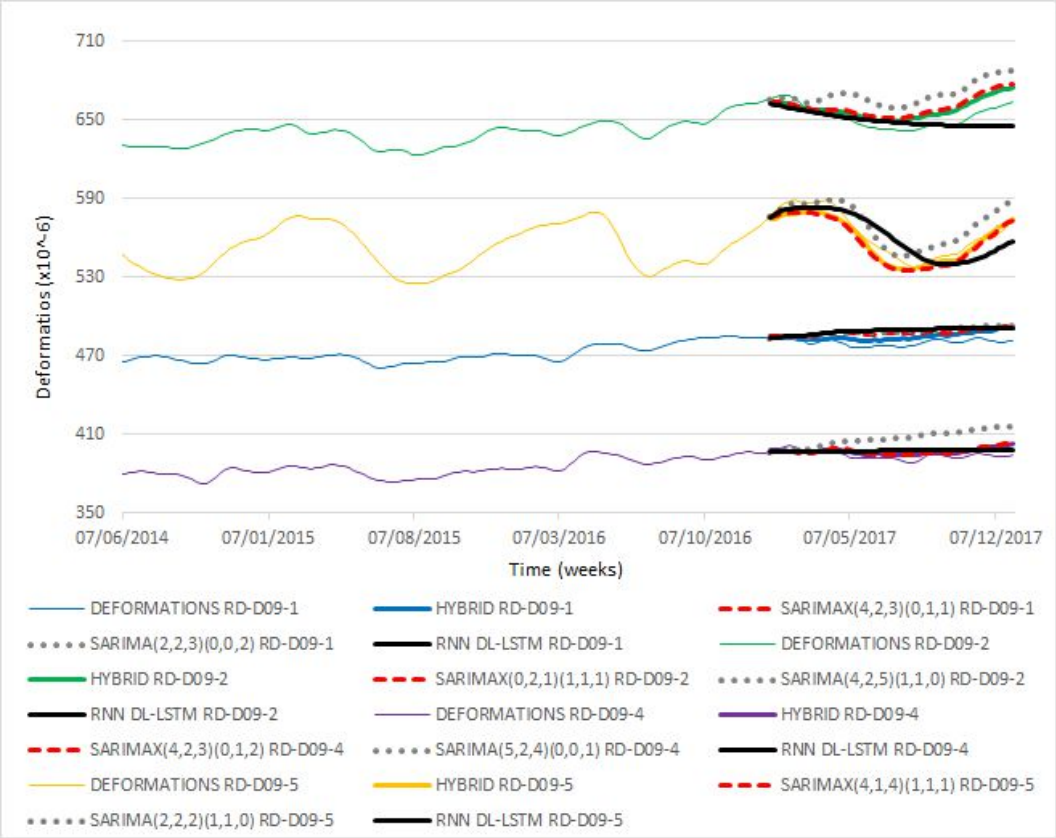

Figure 2 – data and predictions of four rosette branches RD-D09 by methods SARIMA, RNN DL-LSTM, SARIMAX E SARIMAX-NEURAL

The Table 3 presents the comparison of the hybrid method's accuracy of the mean values, i.e., the mean of the values of each statistic from Tab. 2, against the individual methods. Note that the goodness of fit statistics MAE, MAPE and RMSE, of the predictions by the proposed hybrid method were lower than the same statistics of the individual methods' predictions. The percentage gains correspond to how much more accurate the hybrid method was in the predictions relative to the other methods in each statistic (per column).

Table 3 - Comparison of the adherence statistics of the RD-D09 rosette predictions with the respective percentage gains

METHOD	**DEFORMIMETER ROSETTE RD-D09**					
	MAE	**MAPE**	**RMSE**	**Percentage comparison**		
SARIMA	12.65	2.42	14.36	58.77%	59.99%	57.99%
RNN DL-LSTM	6.98	1.32	8.08	25.29%	26.93%	25.30%
SARIMAX	6.88	1.28	7.82	24.20%	24.47%	22.88%
SARIMAX-NEURAL	**5.22**	**0.97**	**6.03**	0.00%	0.00%	0.00%

The Figure 3 summarizes the mean values of the MAE, MAPE, and RMSE goodness-of-fit statistics against each method for the 5 modeled time series of the RD-D09 deformimeter rosette of the D57 buttress block.

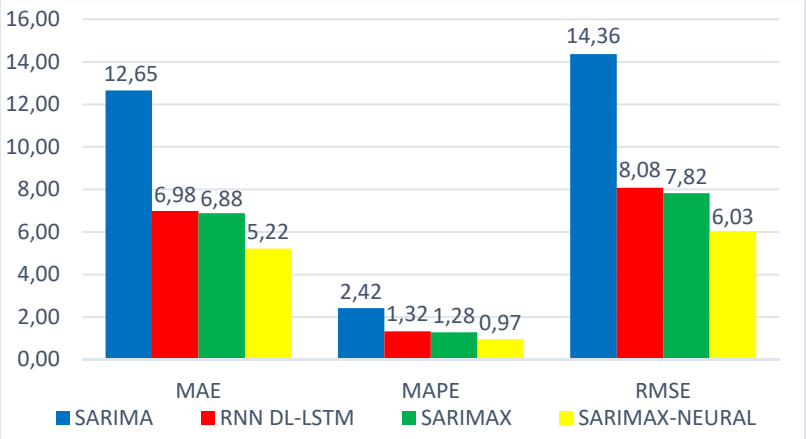

Figure 3 - Comparison of the mean values of the statistics MAE, MAPE e RMSE for 5 time series of the rosette RD-D09

5 Conclusions

It can be stated that by the better prediction accuracy of the hybrid method compared to the individual methods, indeed the ambient temperature has an influence on the corrected concrete strains. This was confirmed by the percentage predictive gain between 25% and 60% over the SARIMA and RNN DL-LSTM methods where the predictions were only on modeling the concrete strains under the effect of ambient temperature.

When comparing the hybrid SARIMAX-NEURAL method with the SARIMAX method, the predictive gain was between 22% and 25%. In this case, the better prediction accuracy was due to the modeling of the SARIMAX residuals by means of the recurrent neural network RNN DL-LSTM, since the hybrid method prediction was defined as the sum of the SARIMAX prediction with the RNN DL-LSTM prediction of the SARIMAX residuals. It is important to highlight that the hybrid method presented in this paper was applied and tested its efficiency in real concrete strain data, in which the respective time series presented seasonality and also with linear and nonlinear self-dependence structure. It is also noteworthy that the hybrid method can be applied to predict other types of instruments that measure different phenomena of concrete, as well as being applicable in other areas of engineering.

Acknowledgements

The authors thank Itaipu for providing the data for this paper.

References

[1] P. K. Mehta and P. J. M. Monteiro, *Concreto Microestrutura, Propriedades e Materias*, 2nd ed. São Paulo: Pini, 2008.
[2] G. Pickett, 'The Effect of Change in Moisture Content on the Creep of Concrete Under a Sustained Load', *ACI J.*, vol. 38, no. 333–56, 1942.
[3] Z. P. Bažant, 'Material Models for Structural Creep Analysis', in *Mathematical Modeling of Creep en Shrinkage of Concrete*, Illinois, USA, 1988, p. 59.
[4] A. M. Neville, *Properties of Concrete*, 5th ed. Pearson, 2011.
[5] H. C. Santos, 'Um Modelo Consistente para Representação da Deformação Lenta do Concreto', pp. 1–10, 2002.
[6] L. T. Kataoka, 'Estudo Experimental e Numérico da Deformabilidade por Fluência e sua Utilização na Monitoração de Estruturas de Concreto', Universidade de São Paulo, São Paulo, 2010.
[7] Z. P. Bažant and S. Baweja, 'Creep and Shrinkage Prediction Model for Analysis and Design of Concrete Structures : Model B3', *Adam Nev. Symp. Creep Shrinkage—Structural Des. Eff.*, vol. 83, pp. 38–39, 2000.
[8] N. J. G. Lockman and M. J, 'Design Provisions for Drying Shrinkage and Creep of Normal-Strength

Concrete', *Am. Concr. Inst.*, vol. 98, no. 2, pp. 159–167, 2001, doi: 10.14359/10199.
[9] 1992-1-1 CEN, 'Eurocódigo 2: Projeto de Estruturas de Concreto - Parte 1-1: Regras Gerais e Regras para Edifícios', p. 245, 2004.
[10] ABNT, *NBR 6118 -Projeto de Estruturas de Concreto - Procedimento*. Rio de Janeiro: Associação Brasileira de Normas Técnicas, 2004.
[11] ACI209.2-R08, 'Guide for Modeling and Calculating Shrinkage and Creep in Hardened Concrete', *American Concrete Institute*, no. Reapproved. p. 48, 2008, doi: 10.1520/C0078.
[12] L. S. Ribeiro, V. E. Wilhelm, É. F. Faria, J. M. Correa, and A. C. P. dos Santos, 'A comparative analysis of long-term concrete deformation models of a buttress dam', *Eng. Struct.*, vol. 193, pp. 301–307, 2019, doi: 10.1016/j.engstruct.2019.05.043.
[13] G. E. P. Box and G. M. Jenkins, *Time Series Analysis Forecasting and Control*. Oakland, 1976.
[14] J. D. Hamilton, 'Time Series Analysis.', *Princet. Univ. Press*, 1994.
[15] G. E. P. Box, G. M. Jenkins, and G. C. Reinsel, *Time Series Analysis: Forecasting and Control*. Englewood Cliffs, NJ: 3 ed, Prentice Hall, 1994.
[16] S. Hochreiter and J. Schmidhuber, 'Long Short-Term Memory', *Neural Comput.*, vol. 9, no. 8, pp. 1735–1780, 1997, doi: 10.1162/neco.1997.9.8.1735.
[17] J. Schmidhuber, 'Deep Learning in Neural Networks: An Overview', 2014. [Online]. Available: https://arxiv.org/pdf/1404.7828v4.pdf.
[18] Y. Bengio, *Learning Deep Architectures for AI*, vol. 2, no. 1. Montreal: Foundations and Trends, 2009.
[19] A. Graves, *Supervised Sequence Labelling with Recurrent Neural Networks*, vol. 385. Toronto: Springer, Studies in Computational Intelligence, 2012.